Nano Energy 70 (2020) 104527

Contents lists available at ScienceDirect

Nano Energy

journal homepage: http://www.elsevier.com/locate/nanoen

Full paper

Direct visualization of dynamic atomistic processes of Cu_2O crystal growth through gas-solid reaction

Zejian Dong [a], Lifeng Zhang [a], Shuangbao Wang [b,**], Langli Luo [a,*]

[a] Institute of Molecular Plus, Tianjin Key Laboratory of Molecular Optoelectronic Sciences, Department of Chemistry, Tianjin University, 92 Weijin Road, Tianjin, 300072, China

[b] School of Physical Science and Technology & Collaborative Innovation Center of Renewable Energy Materials, Guangxi University, Nanning, 530004, China

ARTICLE INFO

Keywords:
Crystal growth
Environmental TEM
Atomic scale
Cu_2O
Gas-solid reaction

ABSTRACT

Crystal growth involves "mysterious" long-range ordering of atoms or molecules through local-only interaction, which requires repeated addition of atoms or molecules to the growing surface from the liquid or vapour phase. Although the canonical theory has successfully explained crystal growth behaviors, detailed atomistic mechanisms, especially for the growth of crystals involving chemical reactions (covalent bond formation), remain mostly elusive. Herein, we reveal such atomistic mechanisms of Cu_2O growth during the oxidation process by real-time atomic imaging in an aberration-corrected environmental transmission electron microscope (AC-ETEM). We directly visualize the atomistic process of sequential bonding between Cu and O atoms onto the growing oxide surface. Besides, we also reveal the unique role of surface defects during the crystal growth process and the effect of growing kinetics on the ending morphology of the oxide crystals. The obtained results provide the fundamental understanding of the crystal growth process and further enrich the metal oxidation theory.

1. Introduction

Crystal growth requires long-range ordering of atoms or molecules to form a rigid lattice through local-only interaction at the growing front, which is often seen as a "black box" process. The classical picture of crystal growth depicts that after random nucleation of critical nuclei, under some degree of supersaturation in gas or liquids, additional atoms or molecules attach one by one, gradually increasing the size of a growing nucleus and the nucleus becomes more stable crystal. Thermodynamically, the free energy of molecules in the solids should be smaller than that in gas or liquids, which is the driving force for crystal growth. However, if the growing crystal has a molecularly smooth surface, it is not energetically favourable to add one molecule because it will has much smaller number of neighbours compared with bulk matrix. The Burton, Cabrera and Frank (BCF) theory [1] proposes local defects such as dislocations on the growing surface to lower the free energy cost compared with that forming a two-dimensional nucleus on a perfect surface, which has been proved experimentally by observing many spiral growth morphologies. However, the BCF theory was not able to cover many routes of crystal growth. For instance, the semiconductor industry achieved large defects-free crystal growth from the melt, and also from ultra-high-vacuum apparatus such as chemical vapour deposition (CVD) and molecular beam epitaxy (MBE). In the later cases, it seems the growth proceeds from a single two-dimensional nucleus on the surface and laterally expanding to cover the whole surface and may be free of dislocations and defects [2]. The seemingly straightforward underlying mechanisms of crystal growth is far from clear especially on the aspect of atomistic processes during nucleation and growth.

The chemical reactions involved non-classic crystal growth process, including growing superlattices structures [3], metal-organic framework (MOF) [4], covalent organic framework (COF) [5] crystals and various transition metal oxides and chalcogenides (TMC) [6] through chemical vapour deposition require chemical bonding formation beside the periodic arrangement of molecules. At the same time, alternative pathways [7] for crystal growth, such as orientation attachment (OA) growth route [8–10], further complicate the underlying mechanisms by introducing pre-nucleation clusters and metastable intermediate clusters as building blocks in crystal growth. All the above new dimensions in understanding the crystal growth process require precise structural

* Corresponding author.
** Corresponding author.
E-mail addresses: sbwang@gxu.edu.cn (S. Wang), luolangli@tju.edu.cn (L. Luo).

https://doi.org/10.1016/j.nanoen.2020.104527
Received 4 December 2019; Received in revised form 10 January 2020; Accepted 20 January 2020
Available online 23 January 2020

and chemical information at the atomic or molecular level in a dynamic manner. Emerging *in-situ* technique based on X-ray [11] and electron [12,13] provide detailed information down to atomic scale and demonstrated aggregation based crystal growth routes. As a versatile *in-situ* characterization technique, aberration-corrected environmental transmission electron microscopy (AC-ETEM) has successfully deciphered mechanisms in vapour phase growth of nanocrystals [14,15] and also provided direct metrics [16] (e.g. direction-specific *van del Waals* interaction between nanocrystals) governing crystal growth. However, direct interpretation of atomistic mechanisms based on these *in-situ* observations is still challenging because of the required extreme spatial and temporal resolution, as well as the missing chemical information.

Herein, we present *in-situ* atomic visualization of a model Cu_2O crystal growth during gas-phase oxidation process, revealing the atom-by-atom mechanisms from the formation of half unit cell 1D to 2D nucleus on existing perfect oxide surface to complete planar to 3D growth of Cu_2O lattice. We also reveal the surface steps or kinks as the possible origin of bulk defects in oxide crystals as well as the kinetic factors governing the morphology of grown nanocrystals.

2. Results and discussion

2.1. Atomistic process of Cu_2O growth

The Cu_2O crystal growth is achieved by *in-situ* thermal oxidation single-crystalline Cu-10at%Au (100) thin films inside the AC-ETEM chamber under an O_2 gas environment. The Cu thin film sample was pre-annealed in H_2 gas under high temperature to generate a clean Cu surface (Fig. S1) and heated at 350 °C under a gas pressure of $\sim 1 \times 10^{-3}$ mbar to enable a stable observation during the oxide crystal growth process. Detailed experimental conditions are described in Supplementary Section 1 and 2. The oxide formed during this condition is identified as Cu_2O phase with a face-centered cubic (FCC) structure through high resolution (HR)TEM imaging and the corresponding FFT image as detailed in Fig. S2. As compared with metallic Cu with a typical FCC structure, Cu atoms in Cu_2O crystal structures still occupy the sites in FCC structures while two O atoms occupy two tetragonal sites in the unit cell and induce a lattice expansion ~17.7% (from 3.61 Å to 4.25 Å) as shown in Fig. S3. We focus on the growing surface of Cu_2O crystal and take videos of HRTEM images with a temporal resolution of 0.2 s.

Fig. 1 shows time-resolved HRTEM images captured from the *in-situ* video (Supplementary Movie 1) of a growing Cu_2O (110) surface from a [001] view direction, depicting the atomistic processes of Cu_2O growth. The detailed structural identification from experimental and simulated HRTEM image and diffraction patterns are shown in Fig. S4. Fig. 1A and B show the nucleation of an adatom column (possibly a 1D atomic chain because of the projection view in TEM) on a stepped surface of the growing oxide. This newly formed adatom column (white arrow in Fig. 1B) has a height of ~1.5 Å (white dashed lines in Fig. 1B), which corresponds to (220) plane distance of Cu_2O. Another adatom column added adjacent to the first column after 1.2 s as shown in Fig. 1C. These observations indicate the Cu_2O crystal growth initiates from the nulceation of a single atomic chain of Cu to a double-chain of Cu adatoms with a sub unit-cell dimension. Further growth involves addition of 2nd layer of Cu atoms through Cu–O–Cu bonding to form a full unit-cell, which proceeds much faster than the previous nucleation event and is not directly visualized here. Nevertheless, the lateral expansion of the as-formed Cu_2O unit-cell is clearly seen that 5 atom columns were registered within 2.4 s from Fig. 1C and D, and additional 4 atom columns were added within 0.6 s from Fig. 1D and E. As shown in the white-dashed-line box in Fig. 1D, this new layer of Cu_2O lattice has a height of 3.0 Å, which includes the whole repeating unit cell. So far, a clear picture of atomistic process of Cu_2O growth as illustrated in the schematic from Fig. 1F–I. Note we use much fewer adatoms (one vs. one column) in the atomic model to better present the chemical reaction and bonding events during the crystal growth. Firstly, surface free Cu atom (green) is

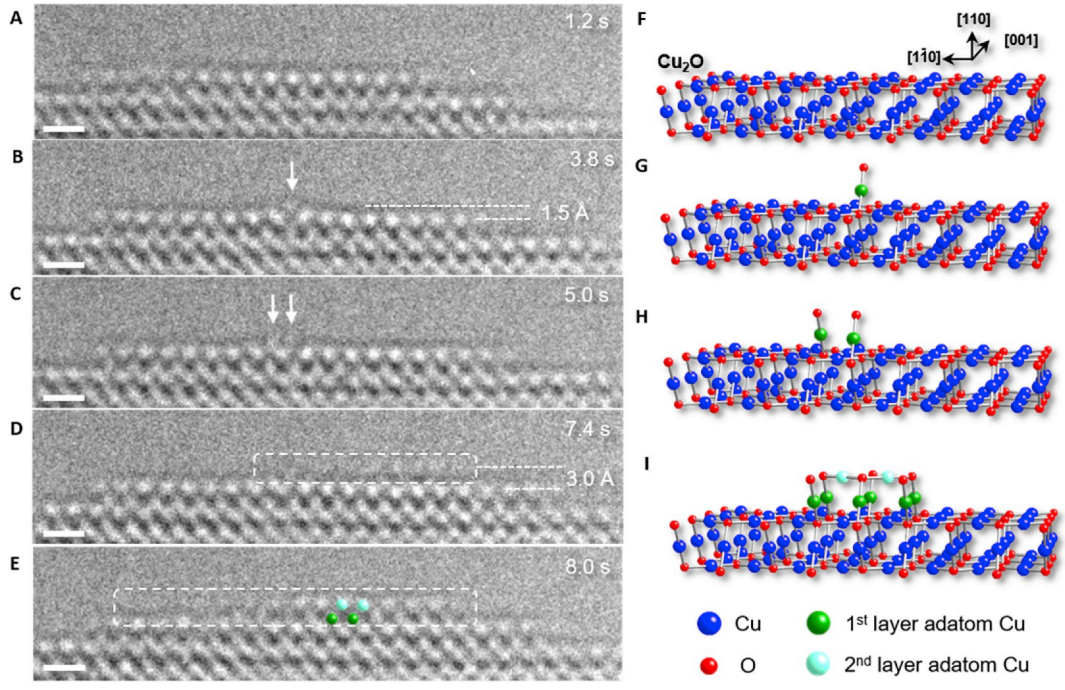

Fig. 1. Atomistic process on a growing oxide surface. (A–E) Time-resolved HRTEM images captured from Supplementary Movie 1, depicting the formation of a new Cu_2O layer on a flat as-grown Cu_2O (110) surface during the oxidation at 350 °C and $pO_2 = 1 \times 10^{-3}$ mbar (A) HRTEM image of initial stepped Cu_2O(110) surface prior to the new oxide layer formation; (B) one Cu atom column (labeled by white arrow) nucleates on oxide surface; (C) another Cu atom column is added adjacent to the first column (another white arrow, they are both 1st layer of Cu adatoms with a step-height of 1.5 Å); (D) incoming Cu and O atoms form the 2nd layer with a step-height of 3.0 Å, completes a whole Cu_2O unit-cell (white-dash rectangular box); (E) The Cu_2O bilayer expands with a clear lattice (white-dash rectangular box); (F–I) scheme of the atomistic process of Cu_2O growth on the surface of Cu_2O(110) corresponding to (A–E). Note that we differentiate 1st layer Cu atoms (green) with 2nd layer Cu atoms (cyan) in (E).

captured by surface O site (bonded with 3 Cu atoms on or below the surface) and possibly bond with another dissociated O atom on the other end as shown in Fig. 1G. When two O–Cu–O surface groups are formed side by side (Fig. 1H), more Cu atoms (cyan) can be captured to form a second layer of Cu in the unit cell (Fig. 1I). During the process above, the formation of the first Cu atomic layer, which is composed of at least two adjacent O–Cu–O groups on (110) surface, seems to be the rate-limiting step as evidenced by different time intervals for nucleation and growth as seen in Fig. 1A–E. These observations highlight the possibility of revealing chemical bonding process in a molecule through only atomic imaging.

Thermodynamically, it is expected that step edges are favoured sites for oxide formation because they could lower the free energy of the system. However, the nucleation and growth of an oxide layer is a process controlled by the interplay of thermodynamic and kinetic factors [17]. The Cu atoms have to diffuse to the reaction front on the oxide surface to grow an oxide layer, leading to the formation of upper terrace. As the upper terrace has a shorter diffusion length compared with the lower terrace, it is possible to nucleate an atom column of oxide on the upper terrace as seen above.

A general "layer-by-layer" growth mode of Cu_2O crystal is shown above although the unit-cell in the adlayer of Cu_2O is consisted of two Cu atomic layers if compared to the crystal growth of pure element such as metals. It is known that crystal growth from solution is actually a dynamic equilibrium procedure, which involves both growth and dissolution of the crystal at the same time [10]. It is interesting to see similar kinetic induced structural fluctuation here for Cu_2O growth during gas phase oxidation reaction (Supplementary Movie 2). As shown in Fig. 2A, an adlayer of Cu_2O with a lateral dimension of ~2.4 nm is grown on the top surface. After 0.2 s, this adlayer shrinks to 2.1 nm losing most of one atom column at its left edge, and the dark contrast with no distinguishable atomic structure (white arrow) seems to track the movement of the surface atoms in Fig. 2B. This indicates the Cu_2O at the step-edge can decompose into smaller building blocks (e.g. surface Cu atoms or Cu–O clusters) and be stabilized in new sites. As we can see in Fig. 2C, a new Cu_2O unit cell is formed a few atom columns away as indicated by the yellow dashed circle. After that, the Cu_2O adlayer grew from 2.4 nm to 4.2 nm by merging new surface sites and old top layer within 0.6 s as seen in Fig. 2D. Note that, it is difficult to completely exclude the effect of other diffusion sources (i.e. surface diffusion or bulk diffusion) during the nucleation of the isolated atom column shown in Fig. 2C. We suggest that these two diffusion sources also largely determine the regrowth process shown in Fig. 2D. It is also worth mentioned that the observation of this decomposition-regrow process is only enabled by a fast-enough camera, which has a temporal resolution higher than this atomic event. An even "faster" frame-rate will certainly enable us to observe more details, especially for surface structural fluctuation, but may introduce more electron beam effect. This intriguing phenomenon is also illustrated in Fig. 2E. Instead of dissolved into the solution, the growing Cu_2O through gas-solid interaction can partially decompose to surface species and atom columns can merge to form larger dimension layers. Hence, this observed decomposition-regrow process resembles the dynamic dissolution-recrystallization process in liquid phase crystal growth and highlights the common ground of crystal growth from gas and liquid environment. Similar phenomenon of oscillatory growth of oxide layer has been reported before [18], where oxygen adsorption on the lower terrace near the step edge could destabilize the oxide layer on the upper terrace.

2.2. Role of defects in Cu_2O growth

Classic BCF theory proposes that surface defects (atomic steps or spiral dislocation) play an essential role in crystal growth and determine the morphology of crystal in some cases, which have been widely recognized and applied to crystal growth practice. In the growth process of Cu_2O, defects can also be generated during chemical bonding and atom arrangements. We directly observed the birth of defects and also found an interesting "memory" effect of defects during the layer-by-layer growth process, where a surface defect can be passed from one oxide layer growth to the next layer. (Supplementary Movie 3).

As shown in Fig. 3A, a metastable 2D nucleus is formed on the top surface of Cu_2O (110) as labeled by the white arrow. After 1.2 s, another stable 2D nucleus (yellow arrow in Fig. 3B) is formed on the left side, which is separated from the previous one by a surface defect (possibly a disarrangement of surface atoms) as labeled by the white arrow. This defect continues to affect the growth of top layer by separating two 2D nuclei on its two sides until a full layer is formed as seen from Fig. 3C–E. However, the defect seems to be healed in the previous top layer (now sublayer) and transferred to the new top layer now (tracked by the white arrow throughout the process). Finally, a new 2D nucleus is formed adjacent to this surface defect (yellow arrow Fig. 3F), which is an identical "inherited" process to that in Fig. 3A. We find this process can be repeated to several layers of Cu_2O growth as shown in Fig. S5.

The schematic in Fig. 3G illustrates the role of surface defect on

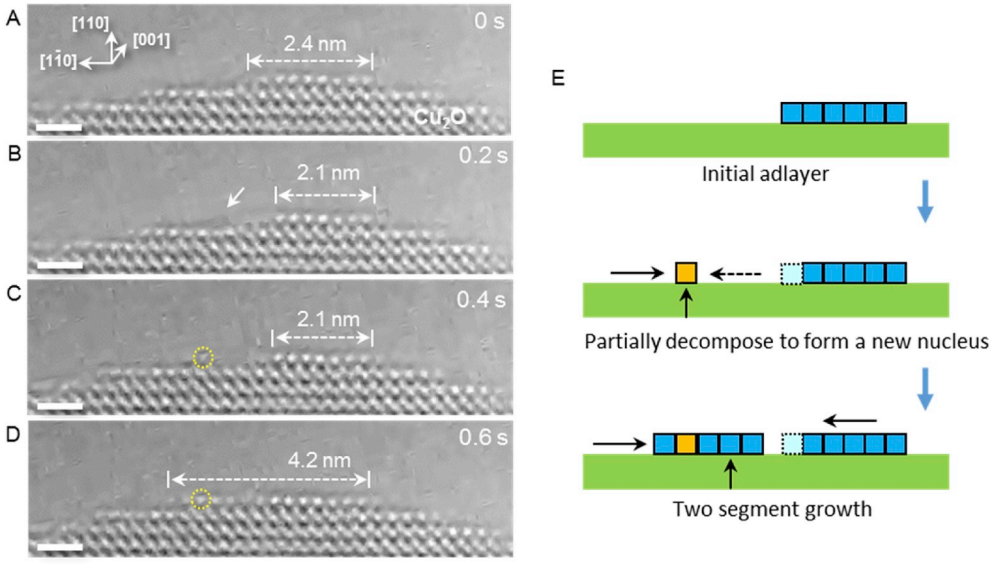

Fig. 2. Atomic scale fluctuation during oxide growth. A two segment growth process is found for the top layer of growing oxide. (A) Initially frame with a 2.4 nm adlayer of oxide, and the left edge of second layer is labeled by a yellow arrow; (B) some atoms (white arrow) decompose from the edge of top layer and partially move to the left side; (C) one atom column nucleates 1 nm away from the outmost layer (the yellow dot circle); (D) more atom columns are added to the existing atom column in (C), and the two segment are nearly connected together; (E) scheme of the two segment growth process. Blue squares label the adlayer while a yellow square labels the new nucleus partially decomposed from the initial adlayer. The light blue square labels the left atom column with a weak contrast after decomposition. The dashed arrow indicates the diffusion pathway of the decomposed atoms while the black arrows denote other possible diffusion pathway (i.e. surface diffusion or bulk diffusion).

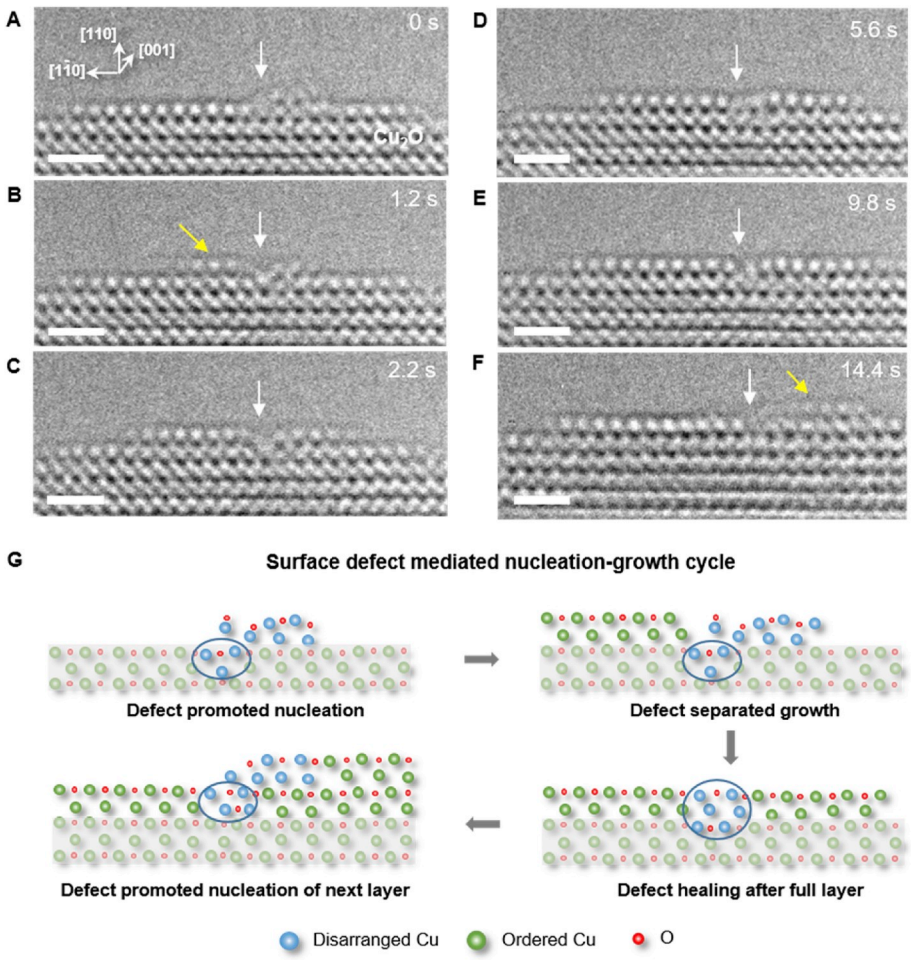

Fig. 3. Defects mediated layer-by-layer growth process. Time resolved HRTEM images depict how a surface defect affects the growth of an adlayer of oxide. (A) a 2D nucleus is formed near a defect (the white arrow); (B) a few atom columns of ordered Cu_2O (yellow arrow) forms on the other (left) side of the defect; (C–E) the defect keeps stable during the propagation on both sides of the adlayer oxide; (F) a new oxide layer forms adjacent to the defect site while the subsurface defect is healed; (G) scheme of the defects mediated layer-by-layer growth process where a surface defect can be passed by a nucleation-growth cycle from one oxide layer to the next layer. The ordered Cu atoms are labeled with green color while the disordered Cu atoms are labeled with blue. The as-grown Cu_2O layer is covered with grey background for better understanding.

layer-by-layer growth, where we highlight how disarrangement Cu atoms (blue balls) around the defect participate in the formation of new layers of Cu_2O in the way of memorizing the position of initial surface defect. Although we cannot determine the nature of the surface defects by imaging, we could see the top layer oxide growth initiates near this site (white arrows in Fig. 3) but cannot grow across it until a full layer growth. It is clear that the surface defect site separates the top layer oxide into two parts as shown in Fig. 3C. Apparently, the energy barrier of growing oxide at the defect is larger than those step-edge sites far away from the defect site within the same layer of oxide growth. However, when it comes to the nucleation of a new top layer, the thermodynamics changes that the nucleation near the defect site is preferred than any other flat surface sites, possibly due to available dangling bonds at the defect site. This is accordance with the observations that the new top layer always nucleate at the defect site (also shown in Fig. S5). The nucleation of new oxide layer is accompanied by the healing of the existing defect, and once the new single atom column is established, the surface defect site becomes no-preferred sites again for the following oxide growth. A loop of "nucleation-at-defects and growth-away-from-defects" is established, and the defect site is passed from previous top layer to the next top layer.

Note that the observed defect is unlikely to be induced by electron beam because only this defect is only occurred in the local position of the sample surface while no more defects are detected throughout our experimental observations. We also anticipate that this effect may lead to the formation of a bulk defect inside the Cu_2O if the surface defect is not healed in time in the sublayer.

2.3. *Growth kinetics and its effect on crystal morphology*

Through real time video recording of HRTEM images, we can investigate the growth kinetics by counting atomic layers/columns formed vs. growth time. Typical time-resolved HRTEM images of Cu_2O with a [110] zone-axis during growth are presented in Fig. 4A–C (Supplementary Movie 4). Generally, the gas-solid growth front exhibits a curved surface (yellow dashed lines) composed of multiple atomic steps. Growth of Cu_2O along both [001] and [1$\bar{1}$1] directions are clearly demonstrated by lattice increment from these images. The similar inset FFT images reveal that there are ignorable changes except for lattice growth. The more and more protruding growth front from Fig. 4A–C indicates that [001] seems as the preferential growth direction compared with [1$\bar{1}$1]. Fig. 4D presents the HRTEM image of Cu_2O through the [110] direction, where the atomic mode and corresponding simulated HRTEM image (insets in Fig. 4D) are well matched with the recorded HRTEM. We measure the layer increment on both [001] and [1$\bar{1}$1] directions from the *in-situ* TEM video as shown in Fig. 4E. A linear growth rate is found for both directions, and the growth rate along [001] is slightly faster than that of [1$\bar{1}$1] direction.

The growth kinetics will have a large influence on the morphological development of the Cu_2O crystal. In Fig. 4F, a "hills-like" growth front with a fast growth rate on [001] direction is observed (Supplementary Movie 4). The atomic structure model and corresponding simulated HRTEM image (insets in Fig. 4D) are matched with HRTEM image. Starting from a flat surface, pile-up of molecules along the normal direction on top of the (001) surface is preferred rather than in-plane lateral growth. This atomistic process will lead to the development of

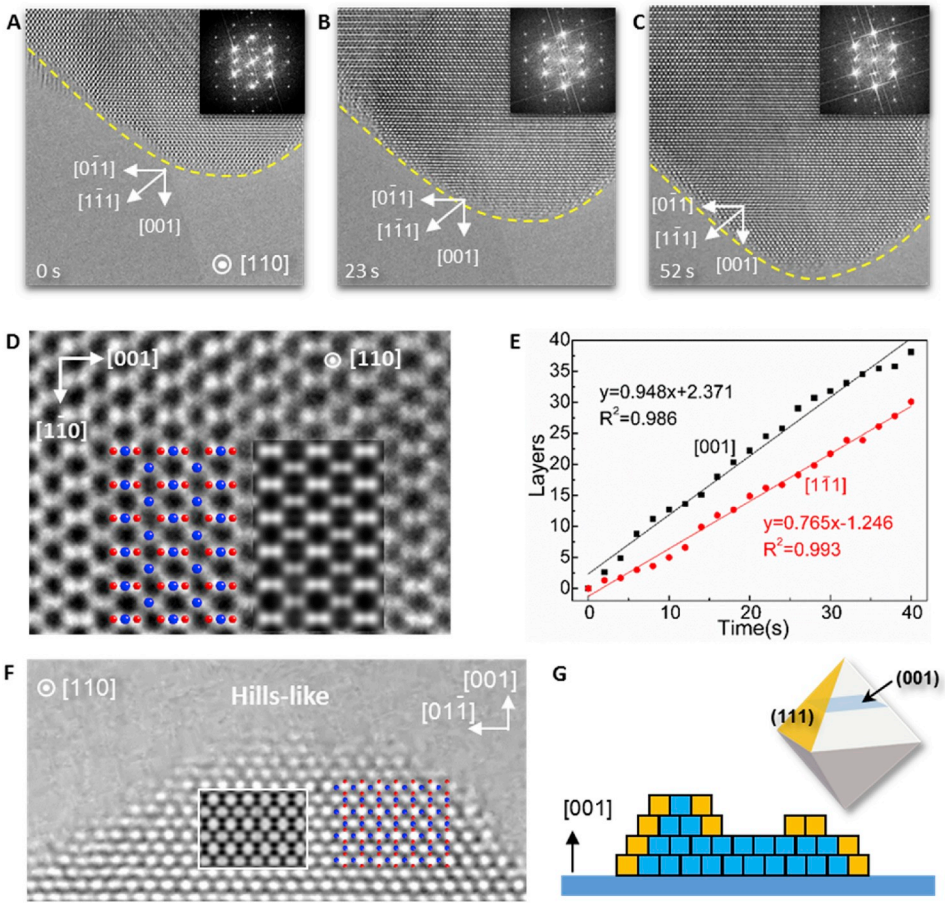

Fig. 4. Growth kinetics of the low-index surface of Cu_2O. (A–C) Time-resolved HRTEM images of atomic growth process of Cu_2O under [110] view direction, the inset pictures show corresponding FFT results; (D) typical HRTEM images of Cu_2O with insets of atomic models and corresponding simulated TEM image. The simulated image is obtained based on the inserted structure model for a specimen thickness of 3.4 nm and a defocus of −14.2 nm; (E) growth rate measured by increment of oxide layers vs. time from the *in-situ* TEM video. The black line shows the growth of the Cu_2O on [001] direction while the red line shows the growth on [1$\bar{1}$1] direction; (F) HRTEM image of a "Hills-like" growth front along [001] direction with the inset of simulated HRTEM image (a specimen thickness of 2.4 nm and a defocus of +12 nm); (G) scheme of the hills-like growth front leads to the final octahedron morphology of Cu_2O crystals.

an octahedron Cu_2O crystal with preferred {111} facets as shown in Fig. 4G. This difference in growth rate for different Cu_2O surface is a balance between a "diffusion factor" that how easy the Cu and O can reach to different surface, and a "surface energy factor" that the arrangement of Cu and O atoms on different crystal planes. As shown in Fig. 4, although it is easier to have Cu atoms diffuse to the (111) surfaces than to the top of convex, the [001] direction is the preferential growth direction. This is because the (111) surface has a higher packing density of surface atoms thus a lower surface energy and is preserved during growth process.

2.4. Mass transport in crystal growth

We have seen that the growth of Cu_2O crystal proceeds through a layer-by-layer mode, which is sustained by atomic transportation to specific sites on top surface. Unlike the crystal growth from a supersaturated solution, where ions are always efficiently supplied surrounding the whole crystal, Cu_2O growth by gas-phase oxidation reaction needs O_2 adsorption and dissociation to supply O atoms and surface and/or bulk diffusion to supply Cu atoms. And these reactant species need to further diffuse to specific sites on tops surface of the growing oxide. Hence, mass transport is a determining factor during these processes. The supply of O can be easily achieved by the bombardment of O_2 gas molecules from the gas environment followed by dissociation and surface diffusion of O on oxide. The diffusion of Cu atoms seems to be a rate-limiting step in the growth process under experimental conditions ($pO_2 = 1 \times 10^{-3}$ mbar and 350 °C) as compared with the supply of O.

There are two major routes for effective Cu atom diffusion, i.e. surface diffusion on the growing oxide and bulk diffusion through the growing oxide. Thermodynamically, surface diffusion is energetically preferred and we did observe addition of atom columns at step edges in Fig. 1. However, the growth of an oxide layer is a process controlled by the interplay of thermodynamic and kinetic factors. Kinetically, it is possible that Cu atoms diffuse to the top of the oxide to form an adlayer through either surface diffusion or bulk diffusion through the oxide lattice. We captured two atomic events representing these two possible diffusion mechanisms mentioned above. Fig. 5A and B show an atomic event within 0.2 s that an atom column disappears near one step edge (yellow circles) while the other two atom columns (white and yellow arrow) are completed from partly occupied to fully occupied status. Given that the step-edge site (yellow arrow) is preferred to be filled by the nearby atom column (yellow dashed circle) with a short diffusion length, the filling of the other atom column far from the step-edge (white arrow) is possibly enabled by a bulk diffusion route through possibly exchange mechanism. As we know, it is usually energetically unfavourable for an atom to diffuse from a lower terrace to an upper terrace by crossing a step edge because of an extra energy cost as E-S barrier [19, 20]. As illustrated in Fig. 5C, cyan coloured Cu atom positions shows one possible diffusion route of a Cu atom from lower terrace to the upper surface. However, we also find another atomic event may not involve bulk diffusion for the similar case of crossing step-edge diffusion. As shown in Fig. 5D, the step edge of the top layer is found to have a relaxed atomic structure comparing with rigid Cu_2O atomic registry. Because the step-edge site Cu atoms have a large chance to have unsaturated coordination with O, which could lead to local structural relaxation as shown by the yellow arrow in Fig. 5D. A "bump" is on the step edge resulting from that Cu atoms deviate from their atomic position. This structural relaxation is restored after 0.2 s as shown in Fig. 5E, but it may create a short-cut diffusion path for Cu to cross the step edge as illustrated in Fig. 5F. It is noted that under elevated temperature used in this experiment, both surface and bulk diffusion of Cu atoms are enhanced.

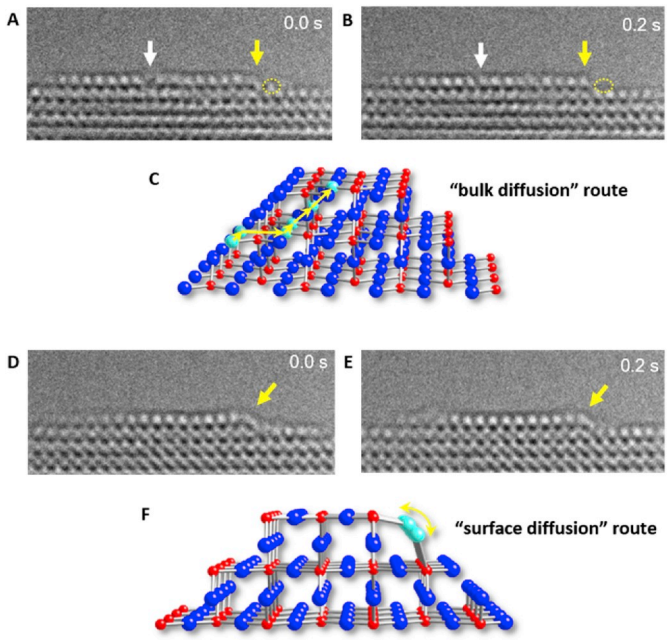

Fig. 5. Possible mass transport routes in crystal growth during gas-solid reaction. (A–B) Time-resolved HRTEM images show a possible atom exchange route for Cu diffusion from lower terrace to upper terrace. The yellow dot circled atom column on a lower terrace disappears while the other two atom columns (labeled by white and yellow arrow) are completely filled within 0.2 s; (C) scheme of a possible diffusion route of Cu atom from a lower terrace to the upper surface; (D) Time-resolved HRTEM images show a "bump" structural relaxation at the step-edge, which could facilitate the mass transport across the step-edge. (E) Restored "bump" structure after 0.2 s, which shows a more regular structure; (F) Structural model of the "bump" structural relaxation leads to Cu atoms surface diffusion across step.

Hence, we see various diffusion routes during the oxidation process.

3. Conclusions

Using AC-ETEM, we directly visualized a growing Cu_2O surface during thermal oxidation reaction in real-time at the atomic scale. We captured the dynamic atomistic process of crystal growth through a bilayer formation of the Cu_2O unit-cell involving sequential Cu–O–Cu bonding. We also find the phenomenon of decomposition and regrowth of top surface oxide layer similar to the dissolution-recrystallization process for solution-based crystal growth. Besides, we reveal the formation of surface defects from the disarrangement of Cu_2O adlayer and its continuing effect on the following crystal growth. Finally, we discuss the growth kinetics and its influence on crystal morphology as well as atomic-scale mass transportation. These microscopic observations not only provide unprecedented details at atomic scale in real-time, but directly related to macroscopic characteristics of crystal growth, which serve as guidelines to crystal engineering. The importance of emerging *in-situ* techniques such as AC-ETEM for deciphering atomistic mechanisms is also demonstrated.

4. Methods

4.1. Cu–Au film growth and TEM sample preparation

The single crystal Cu-10at%Au(100) thin film of ~500 Å was grown on a NaCl(100) substrate by e-beam evaporation. The Cu–Au film was removed from the substrate by floatation in deionized water. After washing, the alloy film was transferred to a MEMS chip and then mounted on an *in-situ* heating TEM specimen holder (FEI® Nano Ex-i/v) for observation.

4.2. In-situ TEM observation

All *in-situ* TEM characterizations were performed in a dedicated field-emission environmental TEM (FEI® ETEM Titan G2 80–300) equipped with an objective-lens spherical aberration corrector. Prior to the *in-situ* oxidation experiments, any native Cu oxide was removed in TEM by heating to 600 °C under H_2 gas flow ($pH_2 \sim 0.1$ mbar). The complete removal of native oxide was then confirmed by electron diffraction (Fig. S1). The *in-situ* oxidation experiments were done after programmed cooling to 350 °C and changing the gas to O_2 ($pO_2 \sim 1 \times 10^{-3}$ mbar).

4.3. HRTEM simulation

All HRTEM simulation (in Fig. 4 and Fig. S4) was done by the SimulaTEM [21] software using the atomic model displayed in each figure. The multislice method was used to calculate the image, which was integrated into SimulaTEM code. The image simulation parameters were chosen as follows: accelerating voltage of 300 kV and a spherical aberration coefficient of the objective lens of 0.01 mm. Other details (i.e. specimen thickness and defocus) are introduced in the manuscript.

Declaration of competing interest

The authors declare that they have no known competing financial interests or personal relationships that could have appeared to influence the work reported in this paper.

Acknowledgments

The authors appreciate the support from the National Natural Science Foundation of China (Grant Nos. 21873069, 11504162) and Thousand Talent Plan Youth Programs of China. The authors appreciate P.K. Shen for the use of the aberration-corrected HRTEM facility.

Appendix A. Supplementary data

Supplementary data to this article can be found online at https://doi.org/10.1016/j.nanoen.2020.104527.

References

[1] W.K. Burton, N. Cabrera, F.C. Frank, The growth of crystals and the equilibrium structure of their surfaces, Phil. Trans. Roy. Soc. Lond. Math. Phys. Sci. 243 (1951) 299–358.
[2] D.P. Woodruff, How does your crystal grow? A commentary on Burton, Cabrera and Frank (1951) 'The growth of crystals and the equilibrium structure of their surfaces', Phil. Trans. Math. Phys. Eng. Sci. 373 (2015) 20140230.
[3] Y. Tian, Y. Zhang, T. Wang, H.L. Xin, H. Li, O. Gang, Lattice engineering through nanoparticle–DNA frameworks, Nat. Mater. 15 (2016) 654.
[4] H. Sung Cho, H. Deng, K. Miyasaka, Z. Dong, M. Cho, A.V. Neimark, J. Ku Kang, O. M. Yaghi, O. Terasaki, Extra adsorption and adsorbate superlattice formation in metal-organic frameworks, Nature 527 (2015) 503.
[5] H. Li, A.D. Chavez, H. Li, H. Li, W.R. Dichtel, J.-L. Bredas, Nucleation and growth of covalent organic frameworks from solution: the example of COF-5, J. Am. Chem. Soc. 139 (2017) 16310–16318.
[6] A. Govind Rajan, J.H. Warner, D. Blankschtein, M.S. Strano, Generalized mechanistic model for the chemical vapor deposition of 2D transition metal dichalcogenide monolayers, ACS Nano 10 (2016) 4330–4344.
[7] J.F. Lutsko, How crystals form: a theory of nucleation pathways, Sci. Adv. 5 (2019), eaav7399.
[8] D.S. Li, M.H. Nielsen, J.R.I. Lee, C. Frandsen, J.F. Banfield, J.J. De Yoreo, Direction-specific interactions control crystal growth by oriented attachment, Science 336 (2012) 1014–1018.
[9] J.J. De Yoreo, P.U.P.A. Gilbert, N.A.J.M. Sommerdijk, R.L. Penn, S. Whitelam, D. Joester, H. Zhang, J.D. Rimer, A. Navrotsky, J.F. Banfield, et al., Crystallization by particle attachment in synthetic, biogenic, and geologic environments, Science 349 (2015).
[10] S. Karthika, T.K. Radhakrishnan, P. Kalaichelvi, A review of classical and nonclassical nucleation theories, Cryst. Growth Des. 16 (2016) 6663–6681.
[11] J.J. Geuchies, C. van Overbeek, W.H. Evers, B. Goris, A. de Backer, A.P. Gantapara, F.T. Rabouw, J. Hilhorst, J.L. Peters, O. Konovalov, et al., In situ study of the

formation mechanism of two-dimensional superlattices from PbSe nanocrystals, Nat. Mater. 15 (2016) 1248.
[12] H.G. Liao, D. Zherebetskyy, H.L. Xin, C. Czarnik, P. Ercius, H. Elmlund, M. Pan, L. W. Wang, H.M. Zheng, Facet development during platinum nanocube growth, Science 345 (2014) 916–919.
[13] M.H. Nielsen, S. Aloni, J.J. De Yoreo, In situ TEM imaging of CaCO3 nucleation reveals coexistence of direct and indirect pathways, Science 345 (2014) 1158–1162.
[14] D. Jacobsson, F. Panciera, J. Tersoff, M.C. Reuter, S. Lehmann, S. Hofmann, K. A. Dick, F.M. Ross, Interface dynamics and crystal phase switching in GaAs nanowires, Nature 531 (2016) 317.
[15] Z. Zhang, Y. Wang, H. Li, W. Yuan, X. Zhang, C. Sun, Z. Zhang, Atomic-scale observation of vapor–solid nanowire growth via oscillatory mass transport, ACS Nano 10 (2016) 763–769.
[16] X. Zhang, Y. He, M.L. Sushko, J. Liu, L. Luo, J.J. De Yoreo, S.X. Mao, C. Wang, K. M. Rosso, Direction-specific van der Waals attraction between rutile TiO_2 nanocrystals, Science 356 (2017) 434–437.
[17] L. Luo, L. Zou, D.K. Schreiber, M.J. Olszta, D.R. Baer, S.M. Bruemmer, G. Zhou, C.-M. Wang, In situ atomic scale visualization of surface kinetics driven dynamics of oxide growth on a Ni-Cr surface, Chem. Commun. 52 (2016) 3300–3303.
[18] L. Li, L. Luo, J. Ciston, W.A. Saidi, E.A. Stach, J.C. Yang, G. Zhou, Surface-step-induced oscillatory oxide growth, Phys. Rev. Lett. 113 (2014) 136104.
[19] R.L. Schwoebel, E.J. Shipsey, Step motion on crystal surfaces, J. Appl. Phys. 37 (1966) 3682–3686.
[20] R.L. Schwoebel, Step motion on crystal surfaces. II, J. Appl. Phys. 40 (1969) 614–618.
[21] A. Gómez-Rodríguez, L.M. Beltrán-del-Río, R.SimulaTEM. Herrera-Becerra, Multislice simulations for general objects, Ultramicroscopy 110 (2010) 95–104.

Zejian Dong received his B.S. from Shandong University in 2013 and his M.S. from the University of Chinese Academy of Sciences in 2018. He is now a Ph. D candidate at the Institute of Molecular Plus & Department of Chemistry, Tianjin University. His research interests mainly focus on exploring the gas-solid interaction between metal alloy/oxide and gas environment by Aberration-corrected Environmental Transmission Electron Microscopy.

Lifeng Zhang received his PhD in the Institute of Metal Research, Chinese Academy of Science. Currently, he is a lecturer at the Institute of Molecular Plus in Tianjin University in China. His current research interest is focused on the advanced (S)TEM studies of microstructure, interface and defects in materials.

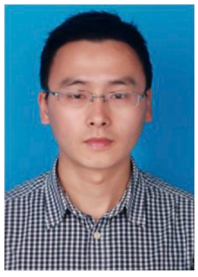

Shuangbao Wang received his PhD in materials science and engineering from the Hunan University. He was a postdoctoral fellow of Nanjing University with prof. Peng Wang. Currently, he is an associate professor at the Guangxi University. His current research interests include the advanced TEM techniques and their applications for some key materials in revealing their related processing, structure and properties.

Langli Luo received his PhD in materials science and engineering from State University of New York at Binghamton. He was a postdoctoral fellow at Northwestern University and Pacific Northwest National Laboratory in USA. Currently, he is a professor at Institute of Molecular Plus at Tianjin University in China. His current research focus on in situ TEM studies of chemical processes and energy related materials.